

# Selective Propene Epoxidation on Immobilized Au<sub>6–10</sub> Clusters: The Effect of Hydrogen and Water on Activity and Selectivity\*\*

Sungsik Lee, Luis M. Molina,\* María J. López, Julio A. Alonso, Bjørk Hammer, Byeongdu Lee, Sönke Seifert, Randall E. Winans, Jeffrey W. Elam, Michael J. Pellin, and Stefan Vajda

Propylene oxide (PO) is an important intermediate bulk chemical that is used in the production of polyurethane and polyols. This product is now commercially produced using either the chlorohydrin or the hydroperoxide routes. Each of these routes has its own limitations,<sup>[1]</sup> owing to the production of undesired chlorinated byproducts or high cost of the H<sub>2</sub>O<sub>2</sub> reactant. A new possibility has arisen based on the experiments performed by M. Haruta et al., wherein small gold nanoparticles were used for the direct propene oxidation by an O<sub>2</sub>/H<sub>2</sub> mixture.<sup>[2]</sup> This new catalyst, if supported on either TiO<sub>2</sub> or titanium silicalite zeolites, converts between 1–10 % propene (depending on the support) with a very high

selectivity (greater than 90 %). Although those results make the use of nanoscale gold very promising, several issues still have to be clarified and improved to employ this catalyst in practical applications. The selectivity of these particles is extremely sensitive to their size and shape, with particles smaller than 1.5–2.0 nm mainly producing propane and particles larger than 4–5 nm assisting oxidation of propene to CO<sub>2</sub> and H<sub>2</sub>O. The other limitation in this reaction is the consumption of hydrogen, which should be as low as possible or, if possible, be suppressed altogether for economical reasons. As the stability of the catalysts should be improved for practical applications, there is a need to study the properties and detailed reaction mechanisms of these catalyst systems, and to look for related new catalysts with improved features.

Herein we present the results of an experimental and theoretical study of the catalytic activity of soft-landed subnanometer gold clusters (Au<sub>6</sub>–Au<sub>10</sub>) for propene epoxidation. Several studies have found a high catalytic activity for similar systems in a number of reactions.<sup>[3]</sup> Interestingly, for small gold clusters, the activity does not seem to depend very strongly on the type of oxide support.<sup>[4]</sup> Irreducible oxides are as good as the reducible oxides as supports, as long as the oxide surface contains defects that serve as traps and activate the catalysts.<sup>[5]</sup> With this in mind, we designed a new type of gold-cluster-based catalyst that is highly active and selective for direct propene epoxidation. The work presented herein comprises the following: 1) amorphous alumina films are used as support instead of the usual titania-based oxides; 2) subnanometer gold clusters are employed instead of larger nanoparticles; and 3) water vapor can replace the expensive and dangerous use of hydrogen in the gas mixture. Ab initio DFT calculations comparing Au/TiO<sub>2</sub> and Au<sub>n</sub>/Al<sub>2</sub>O<sub>3</sub> support the experimental results, assigning a higher activity to the alumina-supported subnanometer gold clusters owing to easier formation of reaction intermediates. The calculations also confirm that different reaction mechanisms take place for both types of catalysts.

The fabrication of the supported gold model nanocatalysts involves several steps. A thin three-monolayer (3ML) alumina film was initially grown by atomic layer deposition (ALD)<sup>[6]</sup> on top of naturally oxidized silicon wafers, providing a rough and amorphous support. Such morphology prevents sintering of the subnanometer catalysts under reaction conditions that usually lead to the loss of highly size-dependent activity and selectivity. Earlier studies confirmed the exceptional stability of the platinum clusters on ALD alumina films.<sup>[7]</sup> A distribution of cationic gold clusters in the range Au<sub>6</sub><sup>+</sup> to Au<sub>10</sub><sup>+</sup> (hereafter referred to as Au<sub>n</sub>) were then

[\*] Dr. L. M. Molina, Prof. M. J. López, Prof. J. A. Alonso  
Departamento de Física Teórica, Atómica y Óptica  
Universidad de Valladolid, 47011 Valladolid (Spain)  
Fax: (+34) 983-423-013  
E-mail: lmolina@fta.uva.es

Dr. S. Lee, Dr. S. Vajda  
Chemical Sciences and Engineering Division, Argonne National  
Laboratory, 9700 South Cass Avenue, Argonne, IL 60439 (USA)

Prof. B. Hammer  
iNano and Department of Physics and Astronomy  
University of Aarhus, Ny Munkegade, 8000 Aarhus C (Denmark)

Dr. B. Lee, Dr. S. Seifert, Dr. R. E. Winans  
X-ray Sciences Division, Argonne National Laboratory  
9700 South Cass Avenue, Argonne, IL 60439 (USA)

Dr. J. W. Elam  
Energy Systems Division, Argonne National Laboratory  
9700 South Cass Avenue, Argonne, IL 60439 (USA)

Dr. M. J. Pellin  
Materials Sciences Division, Argonne National Laboratory  
9700 South Cass Avenue, Argonne, IL 60439 (USA)

Dr. S. Vajda  
Center for Nanoscale Materials, Argonne National Laboratory  
9700 South Cass Avenue, Argonne, IL 60439 (USA)  
and  
Department of Chemical Engineering, School of Engineering &  
Applied Sciences, Yale University  
9 Hillhouse Avenue, New Haven, CT 06520 (USA)

[\*\*] Work supported by Spanish MEC (MAT2005-06544-C03-01) and JCyL (VA017A08) grants. L.M.M. acknowledges support from the “Ramon y Cajal” program. The work at Argonne National Laboratory was supported by the US Department of Energy, BES-Chemical Sciences, BES-Materials Sciences, and BES-Scientific User Facilities under Contract DE-AC-02-06CH11357 with UChicago Argonne, LLC, Operator of Argonne National Laboratory. S.V. gratefully acknowledges the support by the Air Force Office of Scientific Research. B.H. acknowledges financial support from the Danish research councils, FNU, DSF/NABIIT, and DCSC.

Supporting information for this article is available on the WWW under <http://dx.doi.org/10.1002/anie.200804154>.

soft-landed on the alumina film, whilst still keeping surface coverage below 0.03ML to prevent the clusters from sintering. Finally, to fully prevent the clusters from sintering, an additional ALD alumina layer (about 2ML thick) was grown selectively to avoid the overcoating of the supported  $\text{Au}_n$  clusters, leaving them firmly attached at the bottom of a shallow well in the substrate. The reaction experiments were carried out in a reactor by feeding various gas mixtures at 133 kPa ( $\text{C}_3\text{H}_6/\text{O}_2$ ,  $\text{C}_3\text{H}_6/\text{O}_2/\text{H}_2$ , and  $\text{C}_3\text{H}_6/\text{O}_2/\text{H}_2\text{O}$  in helium), and simultaneous X-ray scattering was used to monitor the size of the gold clusters. No change in cluster size, monitored by grazing-incidence small-angle X-ray scattering (GISAXS), was observed over several hours during the experiments, thus confirming that the immobilized gold clusters were resistant to sintering. Sintering was found, however, in the absence of the extra overlayer of alumina.

Figure 1a,b shows the turnover frequency (TOF) for propene oxide and acrolein coproduct formation at various compositions of the gas mixture, as a function of temperature and of reaction time. In all cases, a large activity is found, although qualitative differences are found in the stability. The propene/ $\text{O}_2$  mixture was initially very active at 200 °C, but its activity decreases steadily with time. Adding either  $\text{H}_2$  or  $\text{H}_2\text{O}$  reverses this trend, and the activity slowly increases with time

for  $\text{C}_3\text{H}_6/\text{O}_2/\text{H}_2\text{O}$ . Thus, we can conclude that under steady-state conditions, the presence of surface hydroxy groups at the perimeter of the cluster is crucial. As the reaction proceeds, the surface hydroxy groups are lost, and in absence of  $\text{H}_2$  or  $\text{H}_2\text{O}$  are not replenished at the perimeter of the clusters. Different slopes below or above 100 °C are found in all reactivity plots, suggesting slightly different reaction mechanisms with increasing temperature. Based on the above data, the activation energy for the formation of propene oxide are 26–34  $\text{kJ mol}^{-1}$  and 6–10  $\text{kJ mol}^{-1}$  for the  $T < 100^\circ\text{C}$  and  $T > 100^\circ\text{C}$  regions, respectively. Acrolein production is strikingly different, and for the propene/ $\text{O}_2$  feed there is a high activity, which actually increases with time at 200 °C. With co-fed  $\text{H}_2$ , much less acrolein was formed, and already at 100 °C the production levels off, indicating that excess oxygen in the surface promotes acrolein, whereas the surface hydroxy groups favor propene oxide formation. The most interesting results are found if water vapor is co-fed, for which formation of acrolein is almost completely suppressed.

Plotting the temperature-dependent ratio of propene oxide versus acrolein (Figure 1c), an estimation of the catalyst selectivity is obtained. Without  $\text{H}_2$  or  $\text{H}_2\text{O}$ , we find a 1:2 ratio, whereas selectivity slightly improves with  $\text{H}_2$ , and we obtain ratios between 1:1 and 2:1 depending on the temperature. The most spectacular results are found for water, for which up to 14:1 ratios are observed at 200 °C. This makes propene/ $\text{O}_2/\text{H}_2\text{O}$  an optimal mixture for practical applications of this type of catalyst: the slightly smaller activity for propene oxide production is well compensated by the high selectivity. Copper catalysts also produce propene oxide without hydrogen, although with poorer selectivity.<sup>[8]</sup>

To understand the activity of these new  $\text{Au}_n/\text{Al}_2\text{O}_3$  model catalysts for propene epoxidation and the underlying mechanisms, we performed ab initio DFT simulations of the adsorption of  $\text{C}_3\text{H}_6$  on a model of the alumina-supported small gold nanoclusters. Such supported gold nanoclusters are formed by taking a large slab of the  $\alpha\text{-Al}_2\text{O}_3(0001)$  surface, excavating a hole in it (keeping the slab at 2:3 stoichiometry), and placing a  $\text{Au}_7$  cluster inside, followed by complete relaxation of the structure (Figure 2a). The hole-induced disorder results in significant reconstruction, making the support chemically close to amorphous alumina. In addition, we compare the results obtained with analogous simulations for a model of  $\text{TiO}_2$ -supported gold nanoparticles, which is the prototypical gold catalyst for propene epoxidation.<sup>[2]</sup>  $\text{TiO}_2$ -supported gold nanoparticles are formed by supporting a one-dimensional gold rod on an anatase- $\text{TiO}_2(101)$  slab (Figure 2b). This approach was motivated by the results of Nijhuis et al.,<sup>[9]</sup> which provide evidence for the active interfacial gold-oxide region (also active for CO oxidation)<sup>[10]</sup> that is responsible for the epoxidation reaction between propene and substrate oxygen.

For a more realistic modeling we added a sizable number of hydroxy groups (up to 14), which are likely to adsorb on the alumina surface in presence of  $\text{O}_2/\text{H}_2$  or  $\text{O}_2/\text{H}_2\text{O}$ . Table 1 shows the energetics for the sequential dissociative adsorption of up to seven water molecules on the  $\text{Au}_7/\text{Al}_2\text{O}_3$  model catalyst. Hydroxy groups are easily formed with binding energies of 1–2 eV for the first four pairs and 0.5–1.0 eV for

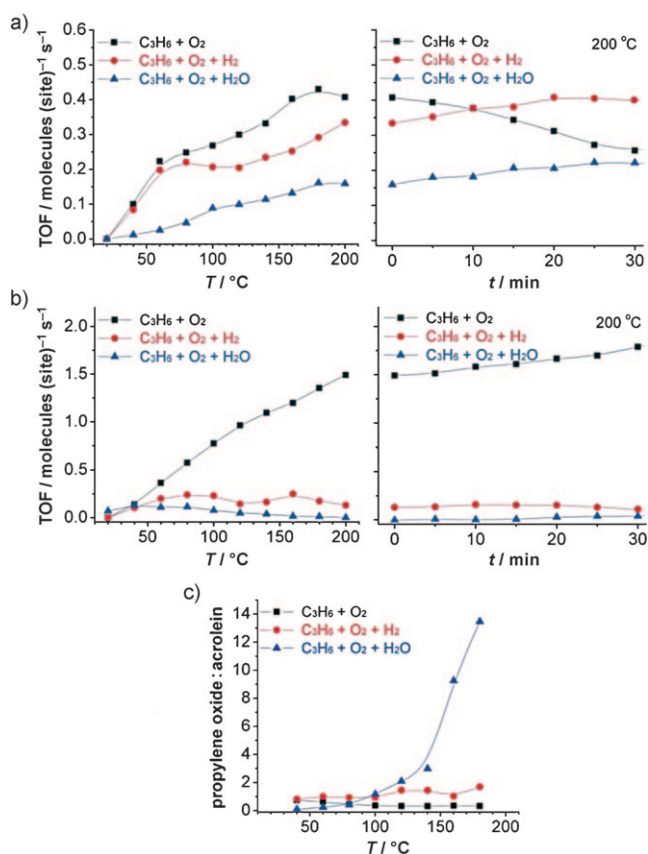


**Figure 1.** a) Propene oxide formation as a function of temperature (left) and time (right, monitored at 200 °C) for various compositions of the gas feed. b) Formation of acrolein as a function of temperature (left) and time (right, monitored at 200 °C) for various compositions of the gas feed. c) Temperature-dependent ratio of propylene oxide to acrolein. ■  $\text{C}_3\text{H}_6/\text{O}_2$ , ●  $\text{C}_3\text{H}_6/\text{O}_2/\text{H}_2$ , ▲  $\text{C}_3\text{H}_6/\text{O}_2/\text{H}_2\text{O}$ .

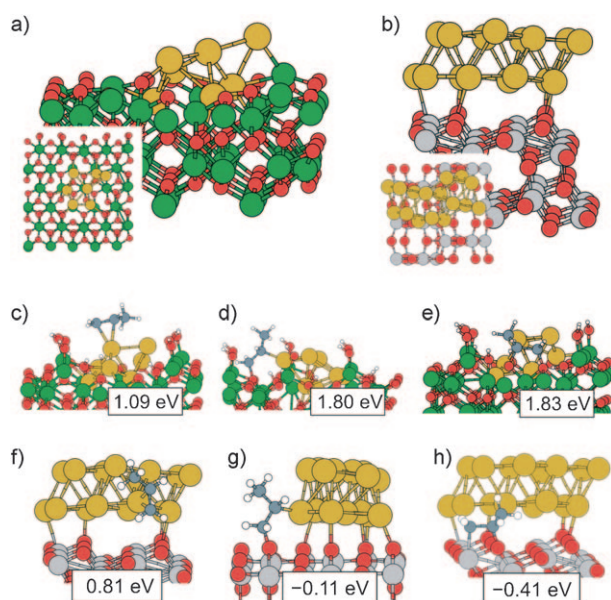


**Figure 2.** Side and top (smaller inset) views of the relaxed structure for the non-hydroxylated a)  $\text{Au}_7/\text{Al}_2\text{O}_3$  and b)  $\text{Au}/\text{TiO}_2$  model catalyst. Most relevant relaxed structures and binding energies (with respect to gas-phase propene) for propene adsorption at c–e)  $\text{Au}_7/\text{Al}_2\text{O}_3$  and f–h)  $\text{Au}/\text{TiO}_2$ . Al green, Au yellow, H white, O red, C gray, Ti light gray.

**Table 1:** Cumulative binding energies (in eV, with respect to water vapor) for dissociative adsorption of up to  $n$  water molecules on  $\text{Au}_7/\text{Al}_2\text{O}_3$ , where  $E_b(n) = nE(\text{H}_2\text{O}, \text{g}) + E(\text{Al}_2\text{O}_3) - E(n\text{H}_2\text{O}/\text{Al}_2\text{O}_3)$ .

$n$	1	2	3	4	5	6	7
$E_b(n)$	2.75	3.57	4.65	6.90	7.56	8.47	8.99

higher coverage, confirming the high reactivity of the surface towards saturation of the dangling bonds.<sup>[11]</sup> In contrast, the  $\text{TiO}_2$  surface is much less reactive; analogous tests provide dissociative binding energies of only 0.5–0.6 eV for the first pair of  $\text{H}_2\text{O}$  molecules. Therefore, a slab with 12 surface hydroxy groups was chosen as the final model for  $\text{Au}_7/\text{Al}_2\text{O}_3$ , which corresponds to the situation in which the adsorption of the hydroxy groups begins to saturate (Figure 2c–e). For  $\text{Au}/\text{TiO}_2$ , the clean system was chosen, as tests in the presence of a single hydroxy group yielded similar propene/propene oxide binding energies.

The results for propene adsorption on both catalysts ( $\text{Au}_7/\text{Al}_2\text{O}_3$  and  $\text{Au}/\text{TiO}_2$ ) are shown in Figure 2c–e and Figure 2f–h, respectively. Three possibilities were found: 1) the adsorption of gas-phase propene onto gold by interaction of the intact double  $\text{C}=\text{C}$  bond and a low-coordinate gold atom (Figure 2c,f). The strong binding (0.81 and 1.09 eV) suggests an easy adsorption, which is in agreement with experiments by Ajo et al. ( $\text{Au}/\text{TiO}_2$ ) and by Nijhuis et al. ( $\text{Au}/\text{SiO}_2$ ), showing that propene binds to gold by  $\pi$  bonding.<sup>[12]</sup> Figure 2d,g shows the diffusion to the gold/oxide interface, which is probably the second step of the reaction and involves the replacement of the double  $\text{C}=\text{C}$  bond by a single  $\text{C}-\text{C}$  bond to form the two new covalent  $\text{C}-\text{surface}$  bonds. In case

of  $\text{Au}_7/\text{Al}_2\text{O}_3$  (Figure 2c,d), the change is almost barrierless, with a highly stable final state (1.5–1.8 eV binding, depending on the site around  $\text{Au}_7$ ). This conformer, which bridges an oxygen surface anion and a gold atom, resembles the metallacycle conformers already found as key intermediates for ethene epoxidation on silver catalysts.<sup>[13]</sup> For the formation of the metallacycle, reactive non-hydroxylated oxygen anions around the gold cluster must exist. Therefore, the removal of the hydroxy group by the interaction with adsorbing  $\text{O}_2$  or  $\text{H}_2\text{O}$  becomes essential. The removal of the hydroxy groups is also aided by the decrease in hydroxy group stability at high coverage found above. We also analyzed the interaction between gold-adsorbed propene and coadsorbed hydroxy groups, which could give rise to the  $\text{C}_3\text{H}_6\text{OH}$  intermediates, but found that there is instead a strong repulsion. In contrast,  $\text{Au}/\text{TiO}_2$  is much more inert to the formation of metallacyclic intermediates (Figure 2g), and although such metallacycles are metastable, they are slightly unstable towards desorption to gas-phase propene.

The third possibility is shown on Figure 2e, in which propene binds to the substrate through two covalent  $\text{C}-\text{O}$  bonds, resembling the bidentate propoxy species recently found during propene epoxidation at  $\text{Au}/\text{TiO}_2$  by Nijhuis et al.<sup>[9]</sup> The stability of the propoxy species is as high as the gold-oxide bridging mode, thus demonstrating that in a small cluster, such as  $\text{Au}_7$ , the  $\text{C}-\text{Au}$  bonds can be as stable as the  $\text{C}-\text{O}$  bonds with the oxide. As for the  $\text{Au}/\text{TiO}_2$  system, Figure 2h shows the most stable metallacycle conformer that forms on the oxide surface, with propene bridging a titanium cation and an oxygen anion (a configuration analogous to the one in Figure 2e is around 0.5 eV less stable). Again, propene adsorbs in a metastable fashion with endothermic binding, confirming the much more inert character of the  $\text{Au}/\text{TiO}_2$  system relative to the  $\text{Au}_7/\text{Al}_2\text{O}_3$  system, which traps propene more efficiently by easy formation of metallacycle propene oxide intermediates. At this point, it is interesting to mention that several very recent experiments<sup>[14]</sup> suggest that the presence of very small  $\text{Au}_n$  clusters could account for the observed activity in nanoparticle-supported gold catalysts on certain reactions. We have analyzed the stability of the conformer in Figure 2g at a  $\text{TiO}_2$ -supported  $\text{Au}_7$  cluster and find an only slightly larger binding energy (0.1–0.3 eV, depending on the coverage by the hydroxy groups; see the Supporting Information), which highlights the qualitative difference between alumina and titania supports.

Structures and energetics for the final reaction step, that is, the formation of propene oxide, are shown in Figure 3. Owing to the differences for propene adsorption, different pathways are explored for either  $\text{Au}/\text{TiO}_2$  or  $\text{Au}_7/\text{Al}_2\text{O}_3$ . For  $\text{Au}/\text{TiO}_2$ , direct surface oxygen removal is not feasible and calls for other sources of reactive oxygen; as extensive simulations of the coadsorption and reaction of  $\text{H}_2/\text{O}_2$  at the  $\text{Au}/\text{TiO}_2$  catalyst show that  $\cdot\text{OOH}$  radicals easily form after reaction of  $\text{O}_2$  with surface hydroxy groups (formed after  $\text{H}_2$  dissociation at the gold nanoparticle),<sup>[15]</sup> which can be perceived as oxidizing agents. Figure 3a shows that after a low 0.5 eV energy barrier, the peroxy radical dissociates and a strongly bound (1.59 eV) propene oxide metallacycle is formed, which can be identified as the bidentate propoxy



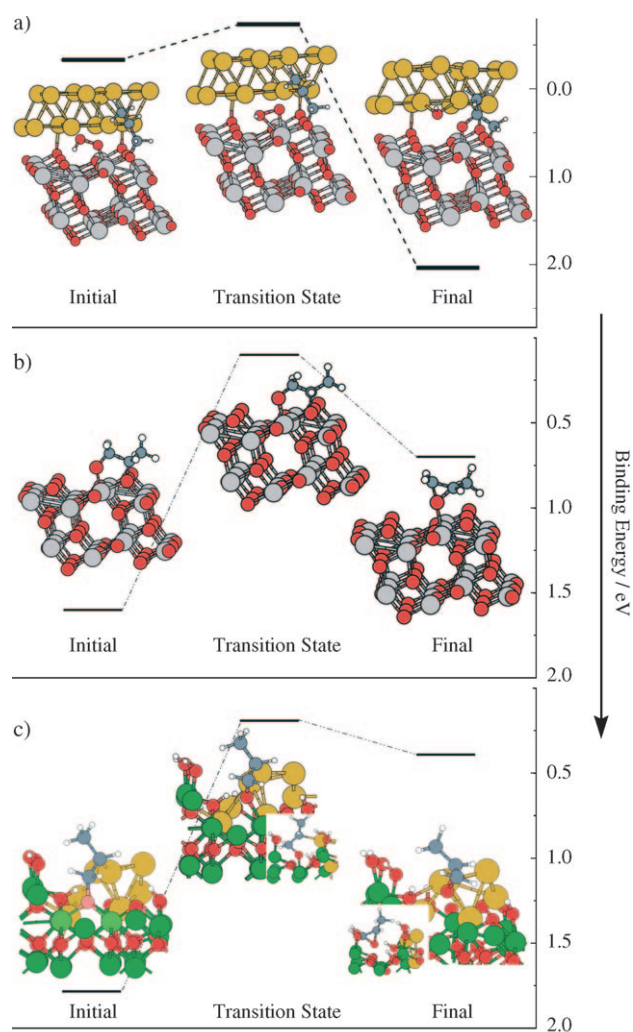


**Figure 3.** a) Structures and reaction energetics for the formation of propene oxide from coadsorbed propene (Figure 2g) and peroxy  $\cdot\text{OOH}$  radicals at  $\text{Au}/\text{TiO}_2$  catalysts. b) Reaction energetics for propene oxide desorption from the anatase  $\text{TiO}_2(101)$  surface. c) Reaction energetics for propene oxide formation at the  $\text{Au}_7/\text{Al}_2\text{O}_3$  model, involving abstraction of substrate oxygen. Insets with rotated views are included for transition and final states. The color code is the same as in Figure 2.

species.<sup>[9]</sup> The last reaction step involves desorption of these species; Figure 3b shows that for  $\text{TiO}_2$  (the gold particle is omitted now, as test calculations show that it does not modify the  $\text{C}_3\text{H}_6\text{O}-\text{TiO}_2$  interaction), this desorption is the most difficult stage of the reaction, taking a moderately high barrier of 1.5 eV to close the metallacycle. The same holds for  $\text{Au}_7/\text{Al}_2\text{O}_3$  (Figure 3c), with a 1.6 eV barrier for substrate oxygen abstraction. The process involves a gradual detachment of the oxygen atom by breaking each of the three  $\text{O}-\text{Al}$  surface bonds: one when the metallacycle is formed, the second in the transition state, and the third during the formation of the second  $\text{C}-\text{O}$  bond in  $\text{C}_3\text{H}_6\text{O}$ . As the process leaves an oxygen vacancy behind, the catalytic cycle will finally be closed by healing it with oxygen.

Comparing the mechanisms for the two systems, some interesting conclusions can be drawn. For  $\text{Au}/\text{TiO}_2$ , reactive

peroxy  $\cdot\text{OOH}$  radicals are needed for the formation of  $\text{C}_3\text{H}_6\text{O}$  metallacycle intermediates, whereas for  $\text{Al}_2\text{O}_3$ -supported gold clusters they can form directly after  $\text{C}_3\text{H}_6$  adsorption. Such differences can be related to the replacement of hydrogen by water in the  $\text{Al}_2\text{O}_3$ -supported catalysts; for  $\text{Au}/\text{TiO}_2$ , we find the dissociation of hydrogen at the gold nanoparticle to be an essential part of the process, both for the formation of the surface hydroxy group and for promoting the adsorption of molecular oxygen with subsequent formation of reactive peroxy radicals. In the case of  $\text{Au}_n/\text{Al}_2\text{O}_3$ , oxygen takes care of “healing” the vacancies (providing either reactive oxygen adatoms, adsorbed hydroxys, or desorbing water, depending on the neighboring hydroxy concentration). Finally, in both cases the presence of neighboring hydroxy groups is probably important for the process of detachment of propene oxide metallacycles from the substrate.<sup>[9]</sup> We expect the calculated energy barriers to be lowered upon inclusion of more coadsorbates, such as water, thus bringing the barriers closer to the measured activation energies (see above). The results shown in Figure 1a (propene/ $\text{O}_2$  atmosphere) can probably be interpreted as arising from a situation in which the hydroxy-terminated surface is transformed into an oxygen-terminated situation, leading to an accumulation of adsorbed metallacycles. These metallacycles are difficult to desorb and block the active catalytic sites.

In summary, the results from the experimental and theoretical study are unexpected and surprising in several ways. First, we demonstrate that our model catalysts based on subnanometer gold clusters are active for the partial oxidation of propene (other similar model catalysts are active for CO oxidation).<sup>[5]</sup> Our work thus complements existing reports on similar activity of larger gold nanoparticles.<sup>[1,2]</sup> Second, to our knowledge, this is the first catalyst for the  $\text{C}_3\text{H}_6/\text{O}_2$  system which uses alumina as support, instead of the commonly applied titania that was considered essential for the production of  $\cdot\text{OH}/\cdot\text{OOH}$  radicals, which are believed to be needed for the promotion of the partial oxidation step on gold/titania. The results from the simulations confirm the viability of this system, assigning an even more active character to the  $\text{Au}_n/\text{Al}_2\text{O}_3$  interface than to the  $\text{Au}/\text{TiO}_2$  one. Third, and more important, for  $\text{Al}_2\text{O}_3$ -supported gold subnanometer clusters the expensive and dangerous hydrogen can be replaced by abundant and safe water vapor, which is also an efficient method to maintain the hydroxy equilibrium at the surface. It will be a challenging task to scale up the production of size-selected clusters by other, more conventional methods, but there are very encouraging experimental efforts demonstrating the feasibility of mass production of supported clusters.<sup>[16]</sup>

## Experimental Section

The beam of gold clusters is produced in a laser ablation source and a distribution of  $\{\text{Au}_{6-10}\}^+$  ions is selected by a mass-spectrometer-quadrupole deflector assembly for deposition.<sup>[17]</sup> Flux and surface coverage upon soft landing are monitored with a picoammeter. The size of the supported clusters is verified by synchrotron grazing incidence small angle X-ray scattering (GISAXS)<sup>[7,17]</sup> before, during, and after the reaction, confirming no aggregation of the subnanometer clusters (see Supporting Information). The studies are performed in a flow reactor at 133 kPa pressure and 30 sccm gas flow.

The reactants used are gases at 1% concentration in helium, their ratio is kept 2:1 for  $\text{C}_3\text{H}_6/\text{O}_2$  and 2:1:1 for  $\text{C}_3\text{H}_6/\text{O}_2/\text{H}_2$  and  $\text{C}_3\text{H}_6/\text{O}_2/\text{H}_2\text{O}$ . Products are detected on a mass spectrometer (Pfeiffer). Turnover frequencies (TOF) are calculated using calibrated gas mixtures and the count of deposited clusters. Activation energies are estimated from the temperature dependence of the TOFs. DFT simulations used a plane-waves basis,<sup>[18]</sup> ultrasoft pseudopotentials<sup>[19]</sup> (scalar-relativistic for gold to take into account relativistic effects), and the Perdew-Wang-91 GGA functional<sup>[20]</sup> for exchange-correlation effects. Transition states and energy barriers are evaluated with a constrained minimization technique.<sup>[21]</sup>

Received: August 22, 2008

Revised: October 29, 2008

Published online: January 16, 2009

**Keywords:** cluster compounds · density functional calculations · epoxidation · gold · propene

- [1] T. A. Nijhuis, M. Makkee, J. A. Mouljin, B. M. Weckhuysen, *Ind. Eng. Chem. Res.* **2006**, *45*, 3447–3459.
- [2] T. Hayashi, K. Tanaka, M. Haruta, *J. Catal.* **1998**, *178*, 566–575.
- [3] P. Pyykkö, *Angew. Chem.* **2004**, *116*, 4512–4557; *Angew. Chem. Int. Ed.* **2004**, *43*, 4412–4456.
- [4] M. M. Schubert, S. Hackenberg, A. C. van Veen, M. Muhler, V. Plzak, R. J. Behm, *J. Catal.* **2001**, *197*, 113–122.
- [5] A. Sanchez, S. Abbet, U. Heiz, W. D. Schneider, H. Häkkinen, R. N. Barnett, U. Landman, *J. Phys. Chem. A* **1999**, *103*, 9573–9578; S. Lee, C. Y. Fan, T. P. Wu, S. L. Anderson, *J. Am. Chem. Soc.* **2004**, *126*, 5682–5683; G. Pacchioni, S. Siculo, C. Di Valentin, M. Chiesa, E. Giamello, *J. Am. Chem. Soc.* **2008**, *130*, 8690–8695.
- [6] J. W. Elam, S. M. George, *Chem. Mater.* **2003**, *15*, 1020–1028.
- [7] R. E. Winans, S. Vajda, B. Lee, S. J. Riley, S. Seifert, G. Y. Tikhonov, N. A. Tomczyk, *J. Chem. Phys. B* **2004**, *108*, 18105–18107; R. E. Winans, S. Vajda, G. E. Ballentine, J. W. Elam, B. Lee, M. J. Pellin, S. Seifert, G. Y. Tikhonov, N. A. Tomczyk, *Top. Catal.* **2006**, *39*, 145–149.
- [8] O. P. H. Vaughan, G. Kyriakou, N. Macleod, M. Tikhov, R. M. Lambert, *J. Catal.* **2005**, *236*, 401–404.
- [9] T. A. Nijhuis, T. Visser, B. M. Weckhuysen, *Angew. Chem.* **2005**, *117*, 1139–1142; *Angew. Chem. Int. Ed.* **2005**, *44*, 1115–1118.
- [10] L. M. Molina, B. Hammer, *Appl. Catal. A* **2005**, *291*, 21–31.
- [11] S. P. Adiga, P. Zapol, L. A. Curtiss, *Phys. Rev. B* **2006**, *74*, 064204; S. P. Adiga, P. Zapol, L. A. Curtiss, *J. Phys. Chem. C* **2007**, *111*, 7422–7429.
- [12] H. M. Ajo, V. A. Bondzie, C. T. Campbell, *Catal. Lett.* **2002**, *78*, 359–368; T. A. Nijhuis, E. Sacaliuc, A. M. Beale, A. M. J. van der Eerden, J. C. Schouten, B. M. Weckhuysen, *J. Catal.* **2008**, *258*, 256–264.
- [13] M.-L. Bocquet, D. Loffreda, *J. Am. Chem. Soc.* **2005**, *127*, 17207–17215; S. Linic, M. A. Barteau, *J. Am. Chem. Soc.* **2003**, *125*, 4034–4035; D. Torres, N. López, F. Illas, R. M. Lambert, *Angew. Chem.* **2007**, *119*, 2101–2104; *Angew. Chem. Int. Ed.* **2007**, *46*, 2055–2058.
- [14] A. A. Herzing, C. J. Kiely, A. F. Carley, P. Landon, G. J. Hutchings, *Science* **2008**, *321*, 1331–1335; M. Turner, V. B. Golovko, O. P. H. Vaughan, P. Abdulkin, A. Berenguer-Murcia, M. S. Tikhov, B. F. G. Johnson, R. M. Lambert, *Nature* **2008**, *454*, 981–983.
- [15] L. M. Molina, M. J. López, J. A. Alonso, B. Hammer, unpublished results.
- [16] B. C. Gates, *Chem. Rev.* **1995**, *95*, 511–522; A. M. Argo, J. F. Odzak, F. S. Lai, B. C. Gates, *Nature* **2002**, *415*, 623–626.
- [17] S. Vajda, R. E. Winans, J. W. Elam, B. Lee, M. J. Pellin, S. Seifert, G. Y. Tikhonov, N. A. Tomczyk, *Top. Catal.* **2006**, *39*, 161–166.
- [18] M. C. Payne, M. P. Teter, D. C. Allan, T. A. Arias, J. D. Joannopoulos, *Rev. Mod. Phys.* **1992**, *64*, 1045–1097.
- [19] D. Vanderbilt, *Phys. Rev. B* **1990**, *41*, 7892–7895.
- [20] J. P. Perdew, J. A. Chevary, S. H. Vosko, K. A. Jackson, M. R. Pederson, D. J. Singh, C. Fiolhais, *Phys. Rev. B* **1992**, *46*, 6671–6687.
- [21] A. Alavi, P. Hu, T. Deutsch, P. L. Silvestrelli, J. Hutter, *Phys. Rev. Lett.* **1998**, *80*, 3650–3653.